3D stereo DIC data from analogue models exploring fault growth and rift propagation in rotational rift systems
(https://doi.org/10.5880/fidgeo.2021.048)

Timothy Schmid[1], Michael Rudolf[2], Guido Schreurs[1], Jürgen Adam[3], Matthias Rosenau[4]

1. *Institute of Geological Sciences, University of Bern, Switzerland*
2. *Institute of Applied Geosciences, Darmstadt, Germany*
3. *Department of Earth Sciences Royal Holloway University, London, England*
4. *GFZ German Research Centre for Geosciences, Potsdam, Germany*

1. License

2. Citation

When using the data please cite:

Schmid, Timothy; Rudolf, Michael; Schreurs, Guido; Adam, Jürgen; Rosenau, Matthias (2021): 3D stereo DIC data from analogue models exploring fault growth and rift propagation in rotational rift systems. GFZ Data Services. https://doi.org/10.5880/fidgeo.2021.048

The data are supplementary material to:
Schmid, T., Schreurs, G., & Adam, J. (2021). Characteristics of continental rifting in rotational systems: New findings from spatiotemporal high resolution quantified crustal scale analogue models. Tectonophysics. https://doi.org/10.1016/j.tecto.2021.229174

Table of contents

3. Data Description

This dataset includes surface 3D stereoscopic Digital Image Correlation (3D stereo DIC) images and videos of 9 analogue models on crustal scale rifting with a rotational component. Using a brittle-viscous two-layer setup, the experiments focused on near-surface fault growth, rift segment interaction and rift propagation. All experiments were performed at the Tectonic Modelling Laboratory of the University of Bern (UB).

All models consist of a two-layer brittle-viscous set up with a total thickness of 6 cm. Thickness variations in ductile and brittle layers are expressed by the ratio R_{BD} = brittle layer thickness/ductile layer thickness, which ranges from R_{BD} = 1 to R_{BD} = 3. The model set up lies on top of a 5 cm thick foam base with a trapezoidal shape with a height of 900 mm and a pair of bases of 310 mm and 350 mm. The foam block is sliced into segments such that 7 interlayered 0.5 cm thick plexiglass bars prevent foam collapse under the model weight. The foam base is initially compressed between the longitudinal side walls and homogeneously expands during the rotational opening. Applied velocities refer to the divergence of the sidewalls at the outermost point (i.e., furthest away from the rotation axis) and decrease linearly towards the rotation axis. These velocities vary from 10 mm/h over a total run time of 4 h up to 40 mm/h over a total run time of one hour, resulting in identical total extension of ca 13% (given an initial model width of 31 cm) for all models. Detailed descriptions of the experiments as well as monitoring techniques can be found in Schmid et al. (2021).

Table 1: *Overview of experiments. Experimental runs also include a model with only the basal foam/plexiglass set up and a model with a basal foam/plexiglass setup and an overlying viscous layer. These two experiments show that the presence of a viscous layer ensures decoupling of the brittle cover from the base setup in brittle-ductile experiments. Models from online-only supplementary material are marked with *.*

Model names in Schmid et al. (2021)	Lab code (UB)	Brittle ductile ratio R_{BD}	Maximum divergence velocity (mm/h)	Monitoring	Comment
Mod_1_10_FOAM*	EXP790	-	-	2D DIC	Foam/plexiglass setup
Mod_1_10_VISC*	EXP799	-	-	2D DIC	Foam/plexiglass setup with viscous layer only
Mod_1_10_REF	EXP800	1	10	3D stereo DIC	Reference model setup
Mod_1_20	EXP992	1	20	3D stereo DIC	
Mod_1_40	EXP993	1	40	3D stereo DIC	
Mod_1_10_CT	EXP822	1	10	3D stereo DIC	CT scanned reference setup
Mod_1_10_EXT	EXP825	1	10	3D stereo DIC	Extensional domain only
Mod_2_10	EXP793	2	10	3D stereo DIC	
Mod_3_10	EXP994	3	10	3D stereo DIC	
Mod_3_20	EXP995	3	20	3D stereo DIC	
Mod_3_40	EXP996	3	40	3D stereo DIC	

3.1. Experiment monitoring

All experiments were monitored by means of top view photographs (DSLR Nikon D-200 10.2 MPx) taken at regular time intervals of 60, 30 and 15 seconds for maximum extension velocities of 10 mm/h, 20 mm/h and 40 mm/h, respectively. In addition, a stereoscopic camera set up of two cameras (2x DSLR Nikon D-810 36.3 MPx) oriented with an angle of about 30° with respect to each other was used to obtain surface elevation and 3D displacement vectors using 3D stereo DIC (Adam et al., 2005). In addition, two experiments were monitored with an X-ray computed tomography technique using a 64 slice Siemens Somatom Definition AS X-ray CT scanner at time intervals of 20 minutes.

3.2. Data analysis

3.2.1. 3D stereo DIC of surface deformation

Digital photographs of the surface were analyzed by means of 3D stereo DIC (Adam et al., 2005) to quantify surface deformation. We used the StrainMaster module from the commercial DaVis 8.4 (LaVision) software at the GFZ, German Research Center for Geosciences, Potsdam, Germany. The procedure included camera calibration for image correction and surface height, static scalar field calculation for topography and calculation of 3D displacement fields at the model surface. We applied a least square matching algorithm with adaptive multi-pass cross correlation with interrogation subsets of 31 by 31 pixels with a 75% overlap. This resulted in surface and displacement calculations with an average reconstruction error of 0.4 and 0.05 mm, respectively. Intervals of incremental displacement calculations are 60, 30 and 15 seconds for 10, 20 and 40 mm/h divergence velocities, respectively. Cumulative displacements are calculated using the Lagrangian sum to account for material advection due to applied boundary conditions (velocities). To ensure that the brittle cover is decoupled from the base setup by the viscous layer (i.e., excluding potential boundary effects due to the basal setup), we run additional 2D DIC analyses on surface top view images of the basal setup as well as the basal setup with overlying viscous layer.

3.2.2. DIC data processing

To read the DaVis proprietary file format .vc7, add-ons for MATLAB as well as Python exist (https://www.lavision.de/de/downloads/software/matlab_add_ons.php). Therefore, further processing requires conversion from .vc7 to Python or MATLAB readable format, for example hierarchical .hdf5 data sets (see *"read_piv.py"* in Michail et al. 2021). For simplicity, we provide DIC test data already in the form of hierarchical .hdf5. The DIC derived 3D displacement fields are further processed with MATLAB (Ver. 2018b) scripts to quantify vertical displacements and subsidence patterns, principal stretching, and growth of single faults of the rift system. The available files are organized in folders (Table 2) with specific functions. In addition, used MATLAB scripts can also be found on https://github.com/TimothySchmid/Characteristics_of_rotational_rifting.git.

DIC data visualization

The folder *DIC_data_visualization* contains MATLAB scripts to visualize displacement and strain maps from DIC data. The .hdf5 files consist of a set of example files for incremental data (incr_test.h5) and cumulative displacement fields (cum_tes.h5). Complete data sets are in the order of several GB and cannot be included here. Plotting variables can be selected from a wide range of displacement derived fields and are listed in the script *"dic_visualize.m"* and stored as .png figures (Fig. 1).

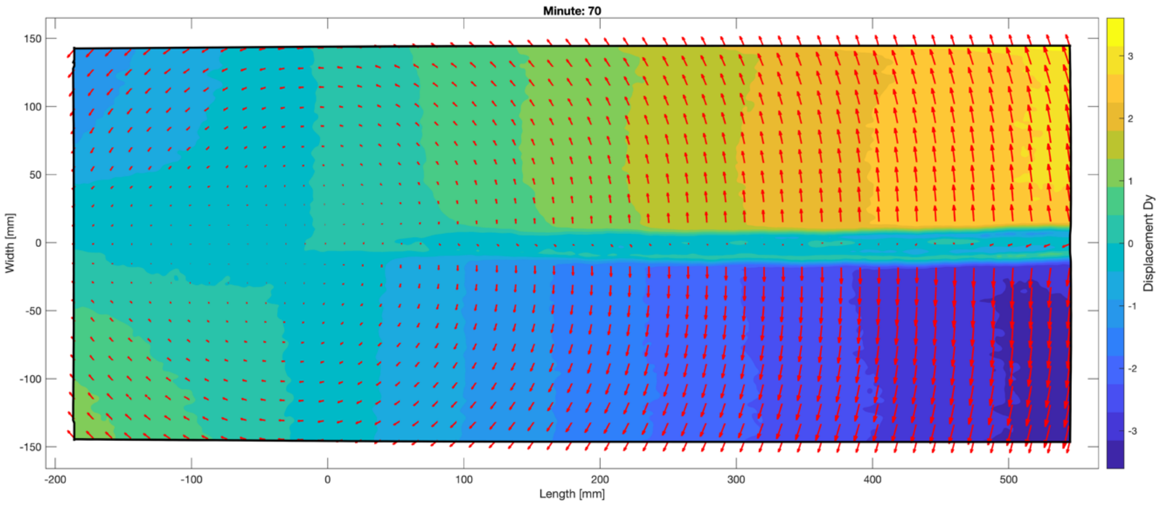

Figure 1: *Output example of the MATLAB script "dic_visualize.m".*

Topographic profile correction

Due to the rigid basal setup, our models are not isostatically compensated and subsequent extension causes homogeneous thinning of the viscous layer resulting in regional subsidence of the model surface. We correct topographic profile lines (extracted from stereo height data in DaVis 8.4 and stored as .txt files) by filtering out such regional subsidence. The MATLAB script "*topographic_profile.m*" considers discrete elevation height data along a profile line as a function of the spatial position x and an arbitrary vertical offset c (f(x) = x + c) indicating the regional subsidence for a given profile line. By applying the difference function (numeric derivative) followed by its inverse cumulative summation function (i.e., improper integral), we back filter out the constant offset c and hence, correct for regional subsidence (Fig. 2). In addition, this method detects potential outliers (due to data holes in the DIC data) in the derivative domain and replaces them before applying the inverse function.

Rift tip tracking

The *"tip_picker.m"* script allows to manually track rift tips of the rift boundary faults over time to estimate rift propagation rates. Furthermore, the *"tip_picker_visualize.m"* script visualizes rift tip positions and growth rates over time (Fig. 3). To generate images where we apply rift tip tracking, we use DIC derived strain maps on which we set a threshold of 10 % strain. Such images can be reproduced with the script "generate_threshold.m" in the DIC data visualization folder.

__Table 2:__ Provided MATLAB scripts for postprocessing of DIC-derived displacements

Folder name	Description
DIC_data_visualization	Visualize and save displacement fields and displacement derivatives from DIC data. Generate threshold images
Topographic_profile_correction	Topographic correction and visualization of topographic profiles over time
Rift_tip_tracking	Manual rift tip tracking of rift boundary faults and plotting of tip position and growth rates over time

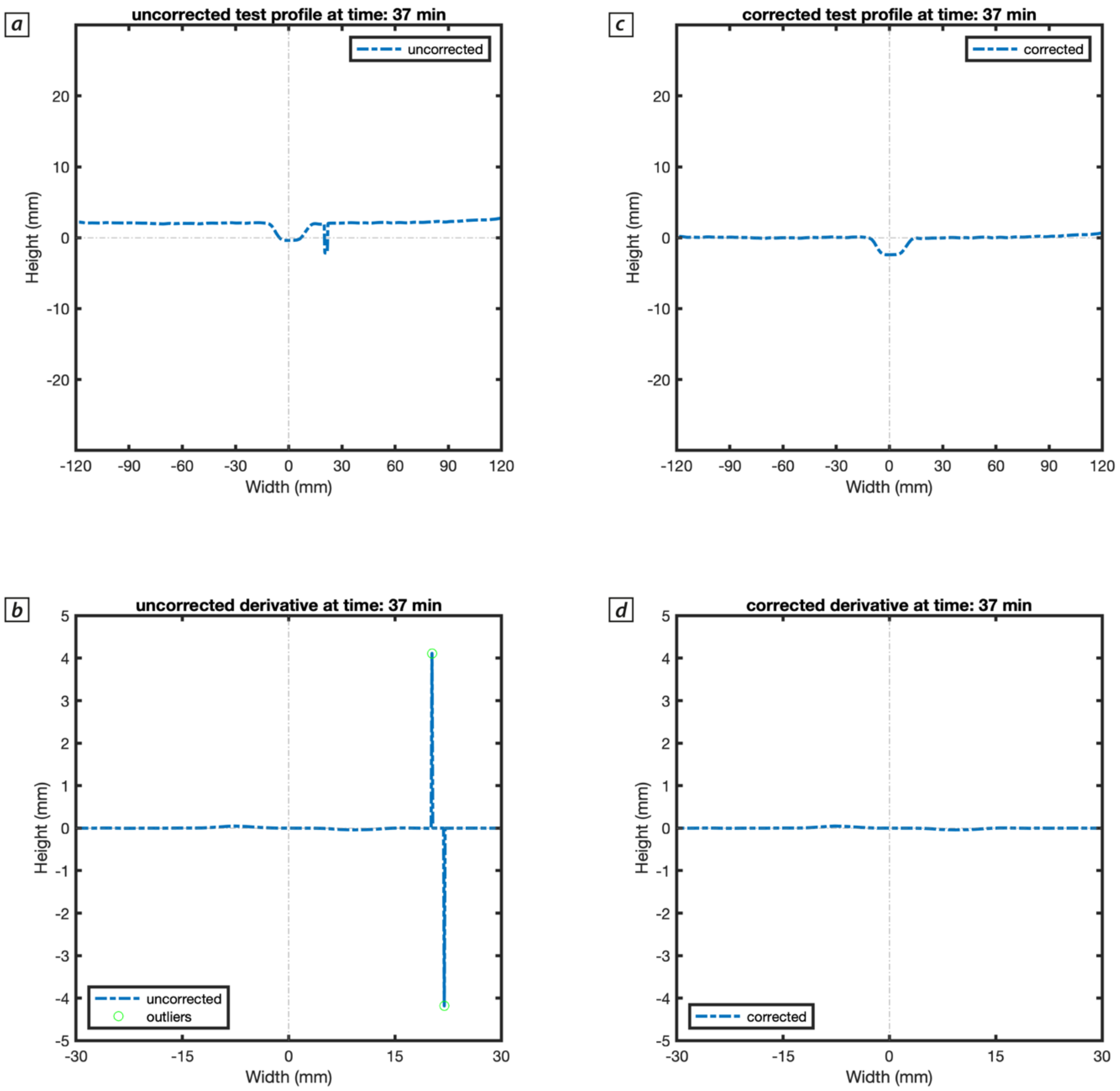

***Figure 2:** Example of topographic profile correction. a) Original topographic cross section of the rift at the final model stage. Note that the overall surface is lower than 0. b) numeric difference profile of the topographic cross section and outlier detection. c) Shift-corrected topographic cross section after cumulative summation of the numeric difference profile in b). d) Numeric difference profile of the corrected topographic profile is identical with the numeric difference profile in b).*

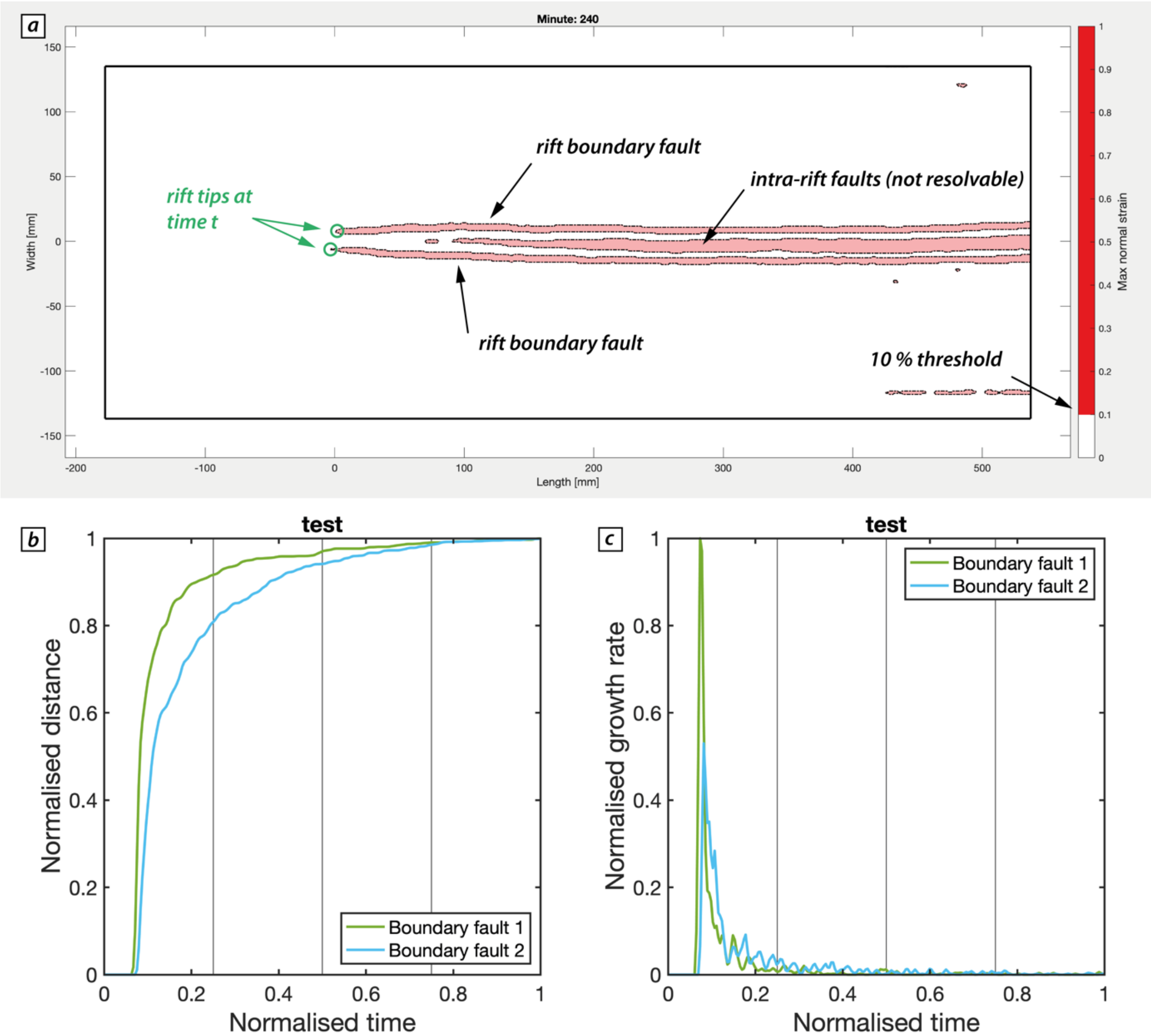

Figure 3: *Example output of the "tip_picker.m" script. a) Maximum normal strain map at the final model stage with a threshold of 10%. The manual rift tip tracking of both rift boundary faults is stored and can be further visualized. b) Normalized rift tip position for both rift boundary faults over time. c) Corresponding normalized growth rates for both rift boundary faults.*

4. Surface deformation videos

The videos for surface deformation evolution show a) top view evolution, b) height evolution data and c) cumulative maximum normal strain (i.e., stretching magnitude) evolution (Fig. 4). Image interval for top view evolution and subsequent 3D stereo DIC analysis is 60, 30, and 15 seconds for 10 mm/h, 20 mm/h and 40 mm/h maximum divergence velocities, respectively and, videos are produced with a frame rate of 30 fps.

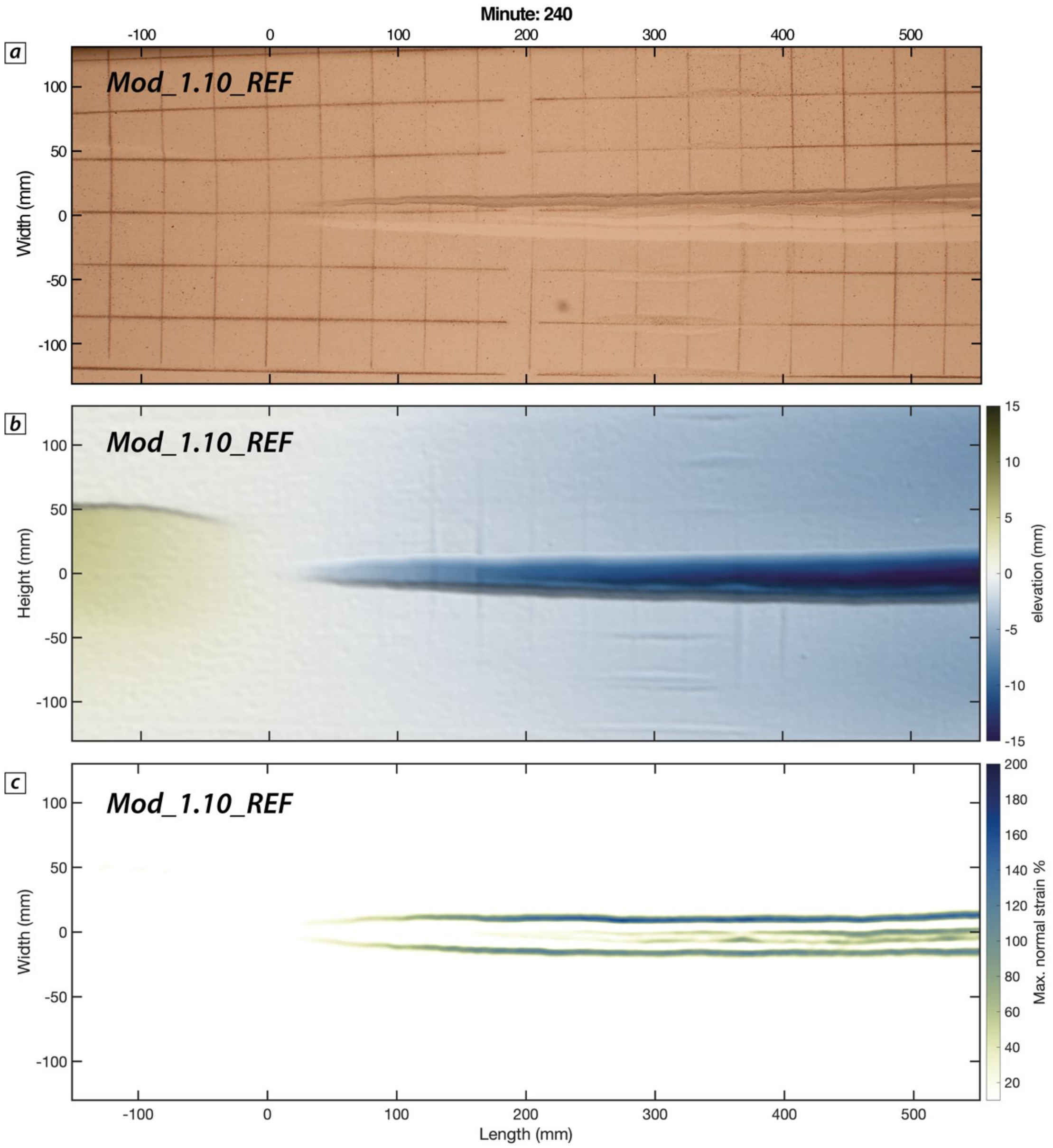

Figure 4: *Example output of movie files of model Mod_1_10_REF. a) Sequence of top view images over the entire model run. b) Sequence of topographic elevation (in mm) evolution. c) Maximum normal strain (i.e., stretching magnitude) sequence in %. Image intervals are 60, 30 and 15 seconds for models with maximum divergence velocities of 10 mm/h, 20 mm/h and 40 mm/h, respectively. All files are stored in separate folders.*

Table 3: *Name convention of videos and images. See List of Files for the complete overview of videos and images.*

Data type	Number	Name convention	Format
Surface top view videos a)	9	ExperimentName_LabCode_topview	.mov
3D stereo DIC obtained height data b)	9	ExperimentName_LabCode_topography	.mov
3D stereo DIC cumulative normal strain c)	9	ExperimentName_LabCode_norm_strain	.mov

5. File description

For each experiment analyzed by means of 3D stereo DIC, the following data are provided:

(i) Surface view videos of the experiments (.mov format)
(ii) Surface height evolution data (.mov format)
(iii) Cumulative normal strain evolution videos of the experiments (.mov format)

An overview of all files of the data set is given in the “2021-048_Schmid-et-al_List-of-Files.xlsx” file.

6. Acknowledgements and funding

The shown experiments were quantitatively analyzed at the HELTEC analogue modelling lab at the GFZ Potsdam within the frame of an EPOS TNA project. We would like to thank Matthias Rosenau and Michael Rudolf for assistance and support during this project. We further thank Kirsten Elger for compiling the data set.

7. References

Adam, J., Urai, J., Wieneke, B., Oncken, O., Pfeiffer, K., Kukowski, N., Lohrmann, J., Hoth, S., Van Der Zee, W., Schmatz, J., 2005. (“Dynamic formation process of thick deformation zone on the ...”) Shear localisation and strain distribution during tectonic faulting—New insights from granular-flow experiments and high-resolution optical image correlation techniques. Journal of Structural Geology 27, 283-301. https://doi.org/10.1016/j.jsg.2004.08.008

Michail, M., Rudolf, M., Rosenau, M., Riva, A., Gianolla, P., Coltorti, M. (2021). Digital image correlation data from analogue modelling experiments addressing magma emplacement along simple shear and transtensional fault zones. GFZ Data Services. https://doi.org/10.5880/GFZ.4.1.2021.004

Schmid, T., Schreurs, G., & Adam, J. (2021). Characteristics of continental rifting in rotational systems: New findings from spatiotemporal high resolution quantified crustal scale analogue models. Tectonophysics. https://doi.org/10.1016/j.tecto.2021.229174